Paleomagnetism of Jurassic carbonate rocks from Sardinia: No indication of post-Jurassic internal block rotations

U. Kirscher,[1] K. Aubele,[1] G. Muttoni,[2] A. Ronchi,[3] and V. Bachtadse[1]

Received 6 April 2011; revised 13 September 2011; accepted 16 September 2011; published 17 December 2011.

[1] Several paleomagnetic studies on Carboniferous and Permian sedimentary and volcanic rocks from Sardinia and Corsica have recently demonstrated (1) the tectonic coherence between southern Corsica and northern Sardinia and (2) significant rotations between individual crustal blocks within Sardinia itself. The geodynamic significance of these rotations, however, is not clearly understood mainly because of uncertainties in defining their timing and causes. In order to contribute to these issues, a pioneering paleomagnetic study on Jurassic carbonates from the Baronie-Supramonte region of eastern-central Sardinia has been extended regionally and stratigraphically. A total of 280 oriented drill cores were taken from 44 sites of Middle and Late Jurassic age in the Nurra, Baronie-Supramonte, Barbagia-Sarcidano, and Sulcis regions. Despite generally weak remanent magnetization intensities, on the order of less than 1 mA/m, thermal and alternating field demagnetizations were successfully applied to define a characteristic remanent magnetization component in about 60% of the samples. Site mean directions show rather good agreement after correction for bedding tilt and yield Middle and Late Jurassic overall mean directions of $D = 269.7°$ and $I = 45.0°$ ($\alpha_{95} = 8.0°$, $k = 14$, and $n = 25$ sites) and $D = 275.5°$ and $I = 50.7°$ ($\alpha_{95} = 7.2°$, $k = 45.3$, and $n = 10$ sites). Positive regional and local fold and reversal tests demonstrate the primary character of the natural magnetic remanence, which is carried by magnetite. These results indicate only insignificant amounts ($\pm 10°$) of post-Jurassic rotations within the island of Sardinia. The resulting Middle and Late Jurassic paleopoles (latitude (Lat) = 16.5°, longitude (Long) = 299.1°, dp = 6.4°, and dm = 10.1° and Lat = 23.4°, Long = 301.2°, dp = 6.5°, and dm = 9.7°), corrected for the opening of (1) the Liguro-Provençal Basin and (2) the Bay of Biscay using rotation parameters from the literature, fall near the coeval segment of the European apparent polar wander path. These results constrain the timing of large differential block rotations found in Late Carboniferous-Permian rocks to a pre–Middle Jurassic age and lead us to exclude tectonics related to the Alpine orogeny for such rotations.

Citation: Kirscher, U., K. Aubele, G. Muttoni, A. Ronchi, and V. Bachtadse (2011), Paleomagnetism of Jurassic carbonate rocks from Sardinia: No indication of post-Jurassic internal block rotations, *J. Geophys. Res.*, *116*, B12107, doi:10.1029/2011JB008422.

1. Introduction

[2] The Paleozoic to Cenozoic tectonic and geodynamic evolution of Sardinia has been studied since the early 1970s. Plate tectonic models based on geologic evidence have been used to relate the counterclockwise rotation of the Sardinia block with respect to Europe north of the Pyrenees, to the opening of the Bay of Biscay [*Van der Voo*, 1969; *Cohen*, 1981; *Olivet*, 1996] during the Aptian [*Gong et al.*, 2008], whereas a wealth of paleomagnetic, radiometric, and marine geophysical data revealed the subsequent counterclockwise rotation of the Sardinia and Corsica blocks during the opening of the Liguro-Provençal Basin in the Miocene [*Alvarez et al.*, 1973; *de Jong et al.*, 1973; *Manzoni*, 1975; *Cohen*, 1981; *Montigny et al.*, 1981; *Vigliotti et al.*, 1990; *Ferrandini et al.*, 2003]. Paleomagnetic data from Permian and Carboniferous rocks of Sardinia [*Zijderveld et al.*, 1970; *Edel et al.*, 1981; *Edel*, 2000; *Moser et al.*, 2005; *Emmer et al.*, 2005, and references therein] revealed the existence of a complex tectonic history characterized by large-scale differential block rotations between individual basins. The origin and geodynamic significance of these differential block rotations observed in Permian rocks of Sardinia are not clearly understood nor is their timing accurately constrained. These rotations may have originated as a consequence of (1) transpressive dextral wrenching related to the late Variscan orogeny [*Edel*, 2000], (2) Late Paleozoic

[1]Geophysics, Department of Earth and Environmental Sciences, Munich University, Munich, Germany.
[2]Department of Earth Sciences, University of Milan, Milan, Italy.
[3]Department of Earth Sciences, University of Pavia, Pavia, Italy.

0148-0227/11/2011JB008422

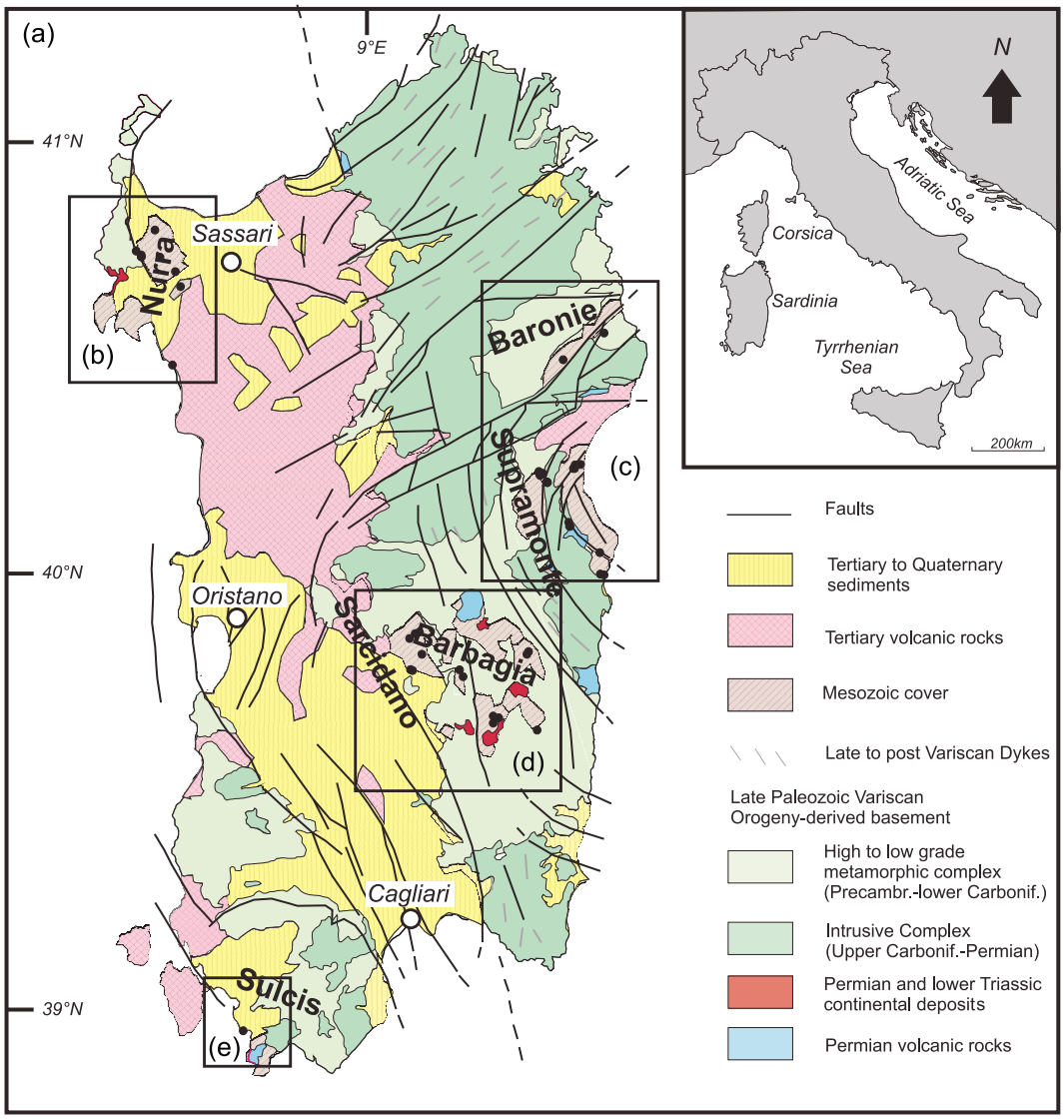

Figure 1. (a) Simplified geological sketch map of Sardinia with major faults and dykes (modified after *Cherchi et al.* [2010]). The four black boxes indicate the study areas: (b) Nurra, (c) Supramonte (Gulf of Orosei) and Monte Albo (Baronie), (d) Barbagia-Sarcidano, and (e) Sulcis. Small black dots represent sampling sites.

post-Variscan shearing between Laurasia and Gondwana [*Arthaud and Matte*, 1977] possibly related to the Pangea B to Pangea A transformation [*Muttoni et al.*, 2003, chapter 5 and references therein], (3) extensional tectonics that characterized the European passive margin during Early and Middle Jurassic times [*Zattin et al.*, 2008], (4) subduction rollback tectonics in the Tyrrhenian Sea since Oligocene times [*Helbing et al.*, 2006], or (5) Cenozoic transcurrent tectonics [*Carmignani et al.*, 1992; *Pasci et al.*, 1998; *Oggiano et al.*, 2009; *Faccenna et al.*, 2002; *Dieni et al.*, 2008]. In order to discern whether these block rotations are Permian features within a dynamic Pangea or are linked to subsequent geodynamic events, a detailed paleomagnetic study has been carried out on well-dated Jurassic sediments from four areas of Sardinia (Nurra, Baronie, Barbagia-Sarcidano, and Sulcis) (Figure 1). This study complements the previous results obtained in the Baronie-Supramonte region by *Horner and Lowrie* [1981].

2. Local Geological Setting and Sampling

[3] The geological record of Sardinia during the Late Carboniferous to Permian is characterized by the emplacement of granitic batholiths, the effusion of volcanic rocks of intermediate geochemistry, as well as the deposition of continental sediments of variable composition [e.g., *Cortesogno et al.*, 1998; *Cassinis et al.*, 1999; *Ronchi et al.*, 2008; *Rossi et al.*, 2009]. Marine sedimentation started in the Middle Triassic with the deposition of Muschelkalk-type limestones [*Posenato et al.*, 2002] and ensued during the Jurassic with various sedimentary units outcropping in the Nurra, Baronie-Supramonte, Barbagia-Sarcidano, and Sulcis areas (Figure 1)

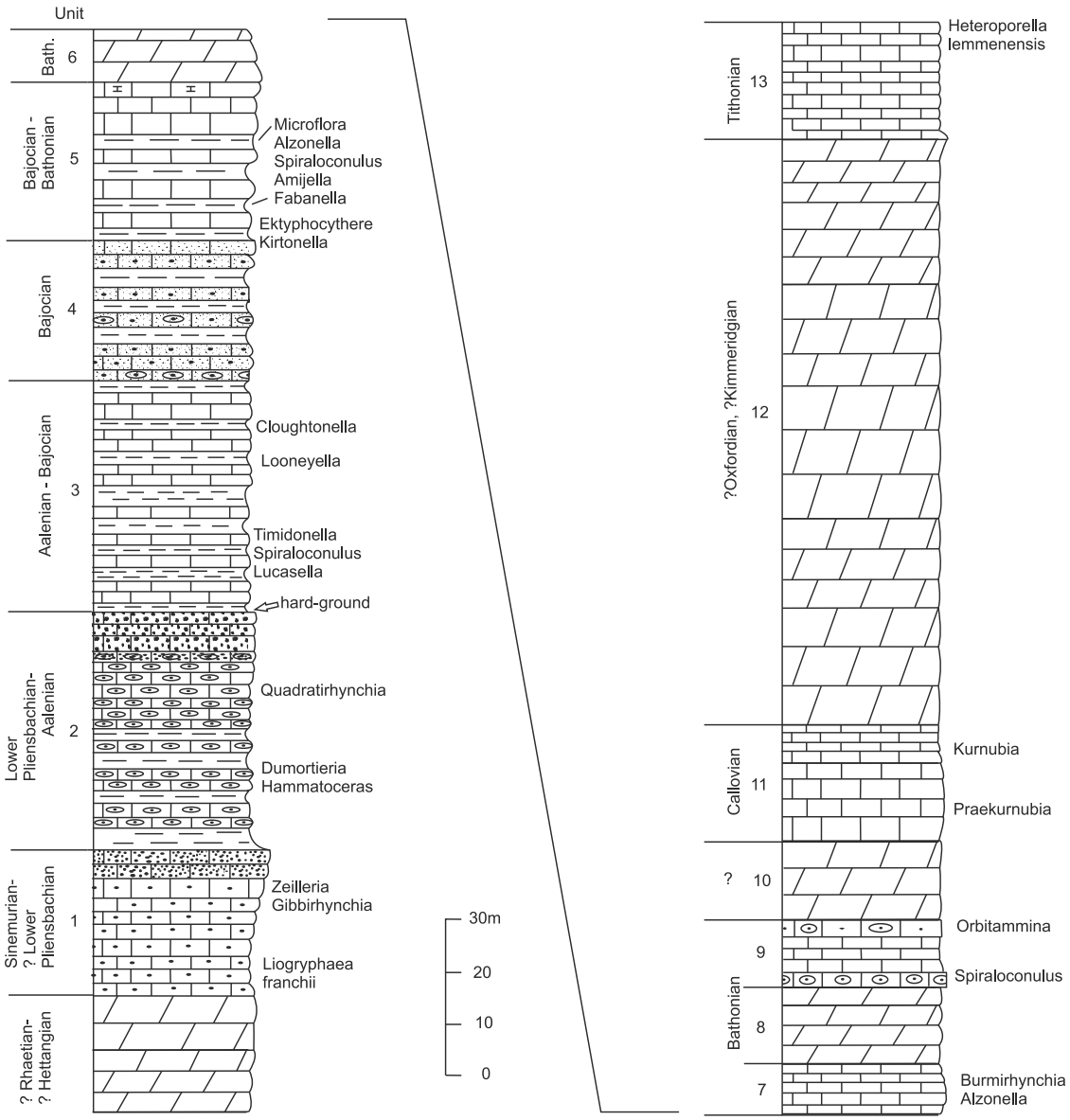

Figure 2. Synthetic stratigraphic section of the Jurassic of the Nurra region (NW Sardinia), modified after *Cherchi et al.* [2010] (numbered units explained therein).

[*Cherchi et al.*, 2010; *Jadoul et al.*, 2010; *Dieni and Massari*, 1986; *Dieni et al.*, 1983; *Costamagna*, 2000].

[4] In the northwestern basin (Nurra), Jurassic sedimentation started with ~50 m of oolitic and bioclastic limestones with at the top reddish sandstones with fossiliferous calcarenites of Early Jurassic age (unit 1 after *Cherchi et al.* [2010]) (Figure 2), followed by 400–575 m of Middle Jurassic oolithic and marly carbonates (units 2–11 after *Cherchi et al.* [2010]) (Figure 2). The Upper Jurassic part of the sequence is composed of 250–300 m of neritic carbonates and micritic limestones extending up to the Cretaceous (units 12 and 13 after *Cherchi et al.* [2010]) (Figure 2).

[5] In the central (Barbagia and Sarcidano) and eastern (Gulf of Orosei) basins, the Variscan basement is disconformably overlain by the Bajocian-Bathonian conglomerates and sandstone of the Genna Selole Formation [*Dieni et al.*, 1983], followed by several hundred meters of Bathonian-Kimmeridgian dolostones and limestones of the Dorgali, Genna Silana, and S'Adde Formations, followed at the top by the Tithonian-Berriasian limestones of the Monte Bardia Formation (Figure 3) [*Costamagna and Barca*, 2004; *Costamagna et al.*, 2007; *Jadoul et al.*, 2010].

[6] The southwestern basin (Sulcis) is characterized by two sedimentary sequences of Mesozoic age [*Barca and Costamagna*, 1997]. The Cala Su Trigu Unit is composed of dolomites and marls with a thickness of ~120 m, indicating deposition in carbonate platform settings. The Guardia Sa Perda Unit, with a total thickness of ~300–350 m, consists of limestones (Punta Tonnara Formation), dolomites (Monte Zari Formation) and marly limestones (Guardia Sa Barracca Formation). They document an evolution from carbonate platform conditions to an environment of middle to outer carbonate shelf (Figure 3). In this paper, we present paleomagnetic data from Middle and

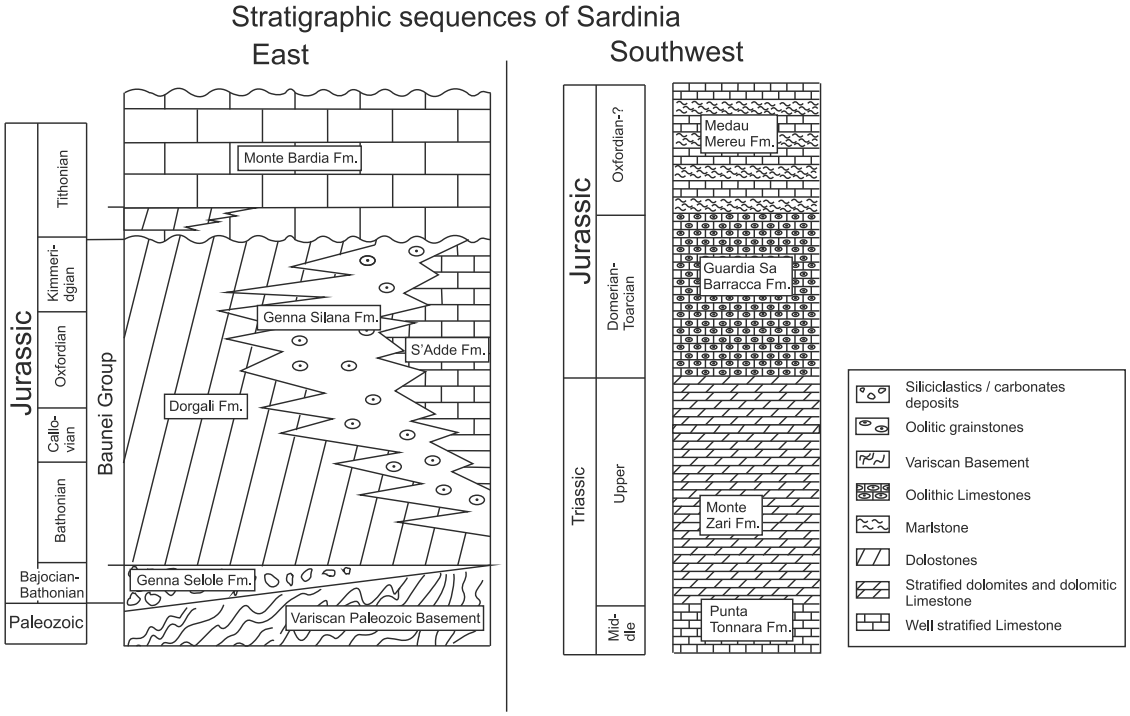

Figure 3. Stratigraphic sections of the Jurassic of central-eastern and southwestern Sardinia, modified after *Costamagna et al.* [2007] and *Barca and Costamagna* [1997].

Late Jurassic sediments from all of the four Jurassic outcrop areas of Sardinia (Figure 1 and Table 1).

3. Field and Laboratory Methods

[7] Paleomagnetic cores were taken in the field using a portable gasoline powered drill and oriented using a standard magnetic compass. All samples were studied in the paleomagnetic laboratory of the University of Munich. Standard ~10 cc cylindrical cores were stepwise demagnetized using thermal (TH) or alternating field (AF) techniques. For TH and AF demagnetization, a Schoenstedt oven and a 2G Enterprises AF device were used, respectively. The magnetization was measured with a 2G Enterprises cryogenic superconducting quantum interference device magnetometer in a magnetically shielded room. Isothermal remanent magnetizations (IRM) were imparted with a magnetic measurements pulse magnetizer with peak fields of 2.3 T. Hysteresis parameters were determined using a variable field translation balance (VFTB) [*Krasa et al.*, 2007].

[8] Demagnetization results were plotted on orthogonal vector diagrams [*Zijderveld*, 1967] and analyzed using the least squares method [*Kirschvink*, 1980] on linear portions of the demagnetization paths defined by at least four consecutive demagnetization steps. The linear fits were anchored to the origin of the demagnetization axes where appropriate.

[9] Only occasionally the combined use of demagnetization great circles and endpoint data [*McFadden and McElhinny*, 1988] was used to retrieve component directions with overlapping coercivity spectra.

[10] Pilot studies demonstrate the superiority of TH on AF demagnetization, and thus the vast majority of the specimens was thermally demagnetized using increments of 30°C in a temperature range from 100°C up to a maximum of 600°C.

4. Results

4.1. Rock Magnetic Results

[11] Rock magnetic measurements were performed on representative samples of the different rock types sampled. Due to the overall weakness of the magnetic signal VFTB experiments turned out to be extremely difficult to perform. However, using also information from IRM acquisition curves, an adequate description of the magnetic carriers of the samples was possible to achieve.

[12] The data were corrected for diamagnetic and/or paramagnetic contributions. In general, the hysteresis loops as well as the thermomagnetic curves show the presence of at least two different magnetic phases with both varying coercivity spectra and Curie temperatures (Figure 4). Important results of these measurements are (1) the presence of a high-coercivity mineral, Curie temperatures (2) in the range of 100 to 150°C (goethite) and (3) at ~550–580°C (magnetite), (4) a hump in the thermomagnetic curves (compare Figures 4e and 4f) starting at ~420°C with a maximum at ~520°C, and (5) an occasional decrease of intensity at ~650°C (Figure 4). The latter can only be observed during "in-field" heating experiments on the VFTB and is attributed to mineralogical alterations during heating such as formation of secondary magnetite from a ferric sulfate phases, which is also indicated by the sharp increase of intensity after cooling to room temperature (Figure 4f).

4.2. Paleomagnetic Results

[13] Detailed thermal demagnetization experiments show the presence of two different magnetic components with

Table 1. Geographic Location of Sampling Sites

Site	Latitude (N°)	Longitude (*E*°)
	Nurra Region	
OLM	40.67522	8.39143
CAS	40.70938	8.37628
CAM	40.74210	8.32900
CCU1	40.75512	8.25665
CCU2	40.74224	8.27200
CCU3	40.74307	8.27193
CCU4	40.80273	8.31397
GRI	40.49788	8.36782
	Sulcis	
MSP	38.99334	8.57973
	Baronie	
SIN	40.57006	9.68499
LUL	40.50956	9.55992
	Supramonte	
OLI1	40.13044	9.57942
OLI2	40.13081	9.58188
OLI3	40.13977	9.57725
ULA1	39.83755	9.44949
ULA2	39.84388	9.45470
RIF1	40.07037	9.67221
CAL	40.27126	9.61375
BAU1	40.02197	9.67358
BAU2	40.01940	9.68568
BUE1	40.26205	9.59512
BUE2	40.27052	9.59682
OHE	40.25556	9.48653
GOR1	40.25151	9.49765
GOR2	40.24687	9.49020
TIS1	40.23105	9.50923
TIS2	40.23157	9.51057
TIS3	40.23021	9.51227
	Barbagia and Sarcidano	
BSM1	39.80065	9.10017
CAN1	39.87437	9.09104
CAN2	39.88484	9.10814
CAN3	39.88891	9.12213
MSA1	39.68027	9.34734
MSA2	39.69184	9.36326
MSA3	39.69615	9.34747
PER1	39.66186	9.41847
PER2	39.66449	9.48054
VNT	39.83845	9.12923
SUL	39.80268	9.09363
SAD	39.80359	9.26015

overlapping unblocking temperature spectra, indicated by the curved shape of some orthogonal vector diagrams (Figure 5). An initial low-temperature component (LTC) with high-intensity values and generally aligned along the present-day field (in in situ coordinates) was removed at low demagnetization temperatures between 100°C up to ~210° C. Eleven sites are characterized by the sole presence of the LTC pointing toward the origin of the projection. The resulting in situ LTC site mean directions are in agreement within error with the present-day field direction for a reference site in central Sardinia, and were therefore excluded from further analysis as they are considered to represent a recent overprint. A high-temperature characteristic component (HTC) of dual polarity broadly oriented to the west and up or east and down in tilt-corrected coordinates was identified as linear segments from ~240°C up to ~600°C in 33 sites. Some ~50% of the samples display unblocking temperatures, which are in a temperature range from 520 to 580°C and are clearly indicative for magnetite. The remaining samples lost all the detectable remanent magnetization at ~450°C, which might be caused by a contamination of the magnetite phase. Samples with different unblocking temperatures, however, do not show different magnetization directions of the HTC (compare Figures 5e and 5f). AF demagnetization was usually not effective in isolating the magnetic components observed during thermal demagnetization experiments. Only occasionally, AF and TH demagnetization experiments yielded comparable results (Figure 5).

4.2.1. Nurra Region

[14] Jurassic rocks of the Nurra region in the northwestern part of Sardinia (Figure 1b) were sampled at eight sites (mostly in the area of Monte Alvaro–Monte Nurra, Table 1). A single site (CCU1) of Early Jurassic age (unit 2 of *Cherchi et al.* [2010] (Figure 2)) did not yield reliable demagnetization results. Four out of a total of six sites of Middle Jurassic age (units 3–5, 8, and 11 of *Cherchi et al.* [2010] (Figure 2)), and one site (OLM) of Late Jurassic age (unit 13 of *Cherchi et al.* [2010] (Figure 2)), are characterized by weak but stable HT component directions (Table 2).

[15] Basically, only two of these sites (OLM, GRI) show statistically reliable results including demagnetization data of more than two samples. The additional three sites of Middle Jurassic age (CAM, CCU3, CCU4) are based on only one or two samples, which show reliable demagnetization behavior. However, their results were included in the calculation of the mean directions only because of their broad coherence with the two trustable sites and because of the good quality of these individual samples.

[16] Because of homogeneous bedding attitudes, no fold test was possible to perform. However, one site where normal and reversed polarities of magnetization were observed (CAM, unit 3, Figure 2) passes the reversal test, classified as C according to the criteria of *McFadden and McElhinny* [1990], whereas the other sites show only normal polarity characteristic components.

[17] The mean direction for rocks of Middle Jurassic age in the area is $D = 259.4°$, $I = 43.4°$, $\alpha_{95} = 27.7$, $k = 12.0$, $n = 4$ sites (Tables 1 and 2), for sites of Late Jurassic age in the area is $D = 243.4°$, $I = 58.3°$, $\alpha_{95} = 14.5$, $k = 29.0$, $N = 5$ samples (Tables 1 and 2).

4.2.2. Supramonte (Gulf of Orosei) and Baronie (Monte Albo)

[18] In the Orosei Gulf area of Supramonte (Figure 1c), two parallel and continuous mountain ridges, composed of carbonates mostly of Jurassic age, extend from north to south exhibiting an overall curvature with radius on the order of ~30 km and convexity facing the Tyrrhenian sea in the east. Thirteen of the nineteen sites sampled in the Dorgali and S'Adde Formations of the Supramonte show the presence of a dual polarity characteristic HT component. To the North of the Supramonte area, starting from the town of Siniscola, another ridge of Jurassic rocks (Monte Albo) extends ~20 km in a southwestward direction. Only two sites were accessible for sampling in this area. Site SIN in the S'Adde Formation yielded characteristic HTC directions. Site LUL consisting of sandy carbonates of the Dorgali Formation (Bathonian after *Jadoul et al.* [2010] or Bathonian-

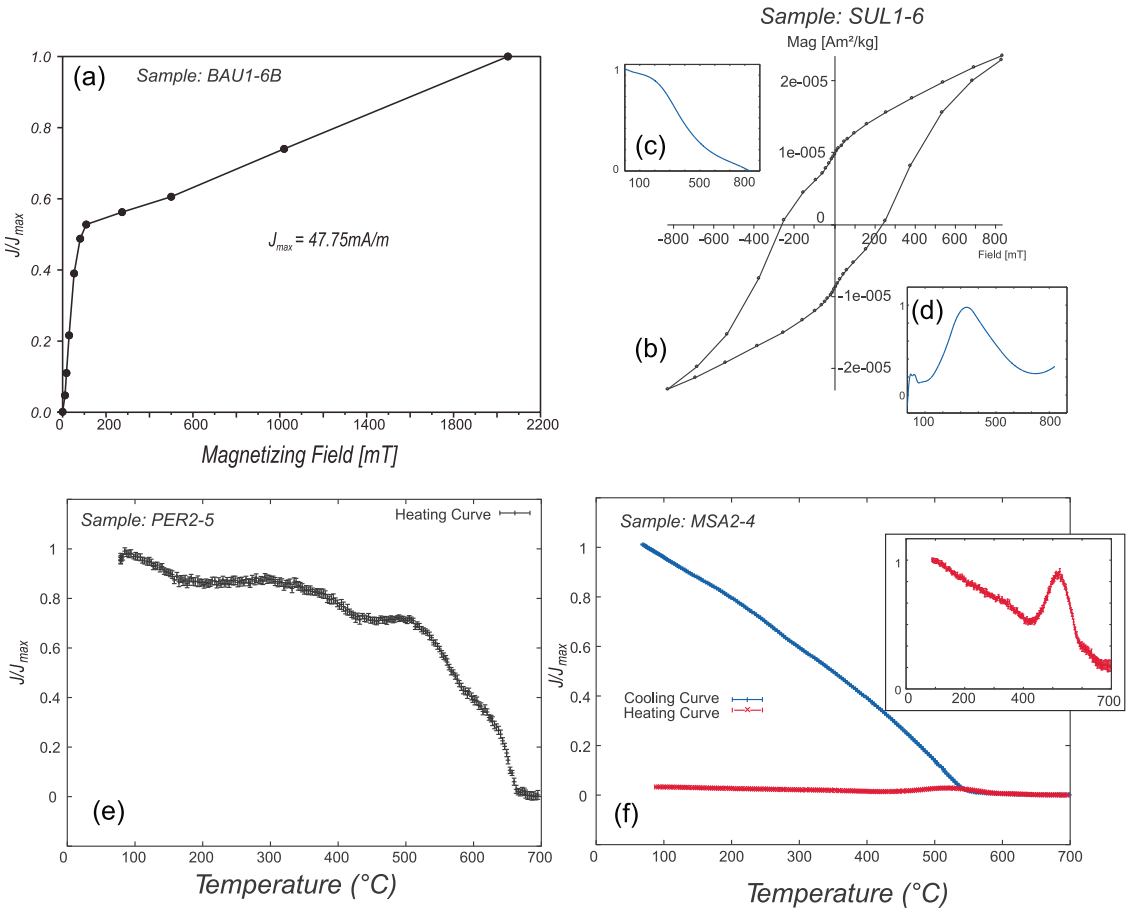

Figure 4. Rock magnetic analysis of representative samples of (a) isothermal remanent magnetizations acquisition curve and (b) hysteresis loop, measured after heating to 150°C. Also shown are the difference of the descending and ascending branches of the (c) hysteresis loop for positive field values and (d) the first derivative of the latter. (e and f) Thermomagnetic curves. In Figure 4f both heating and subsequent cooling curves are shown. Inset in Figure 4f shows only the normalized heating curve with the same axis.

Kimmeridgian after *Costamagna et al.* [2007]) is characterized by very weak magnetizations; two samples from this site yielded stable component directions oriented along the present-day field in in situ coordinates, whereas two other samples treated with the great circle analysis [*McFadden and McElhinny*, 1988] yield an intersection close to the HTC site mean direction of site SIN. In summary, sites from Supramonte and Baronie show similar HTC directions (Table 3). Both mean in situ HTC directions show no similarity with the direction of the present-day field and are thought to reflect primary magnetizations.

[19] Grouped according to age, Late Jurassic site mean directions of the area show an increase of the Fisher precision parameter k [*Fisher*, 1953] from 14.3 to 60.4 after 100% tilt correction. Middle Jurassic site mean directions show no substantial changes of the precision parameter k, which can be explained by rather similar bedding characteristics of these sites (dip directions of 60° to 100° and dips of 15° to 35°).

[20] The mean direction for rocks of Middle Jurassic age in the area is $D = 277.1°$, $I = 41.2°$, $\alpha_{95} = 15$, $k = 14.6$, $n = 8$ sites (Tables 1 and 3). The mean direction for rocks of Late Jurassic age in the area is $D = 278.2°$, $I = 49.4°$, $\alpha_{95} = 6.7$, $k = 60.4$, $n = 9$ sites (Tables 1 and 3).

4.2.3. Barbagia-Sarcidano Region

[21] In the Barbagia and Sarcidano regions, i.e., in the area of the towns of Isili, Laconi, and Nurri (Figure 1d), twelve sites were sampled in Middle Jurassic sediments of the Dorgali Formation. Three of these sites were rejected due to a strongly developed present-day LTC overprint or because of the poor quality of the demagnetization data. The remainder of the sites yields well-defined dual polarity HT component directions (Table 4). At eight sites, these directions pass the reversal test in tilt-corrected coordinates (classified C after *McFadden and McElhinny* [1988]). The tilt-corrected Middle Jurassic mean direction for the area is $D = 273.2°$, $I = 49.7°$, $\alpha_{95} = 12.3$, $k = 13.2$ and $n = 12$ sites (Tables 1 and 4).

4.2.4. Sulcis Region

[22] In the far southwestern part of the island (Figure 1e), to the west of the Campidano graben, Jurassic rocks are only exposed immediately to the north of the village of Porto Pino. In this area, 9 samples in a small-scale syncline in the Medau Mereu Formation (Middle Jurassic after *Costamagna* [2000]) were collected. Eight of these samples yield usable

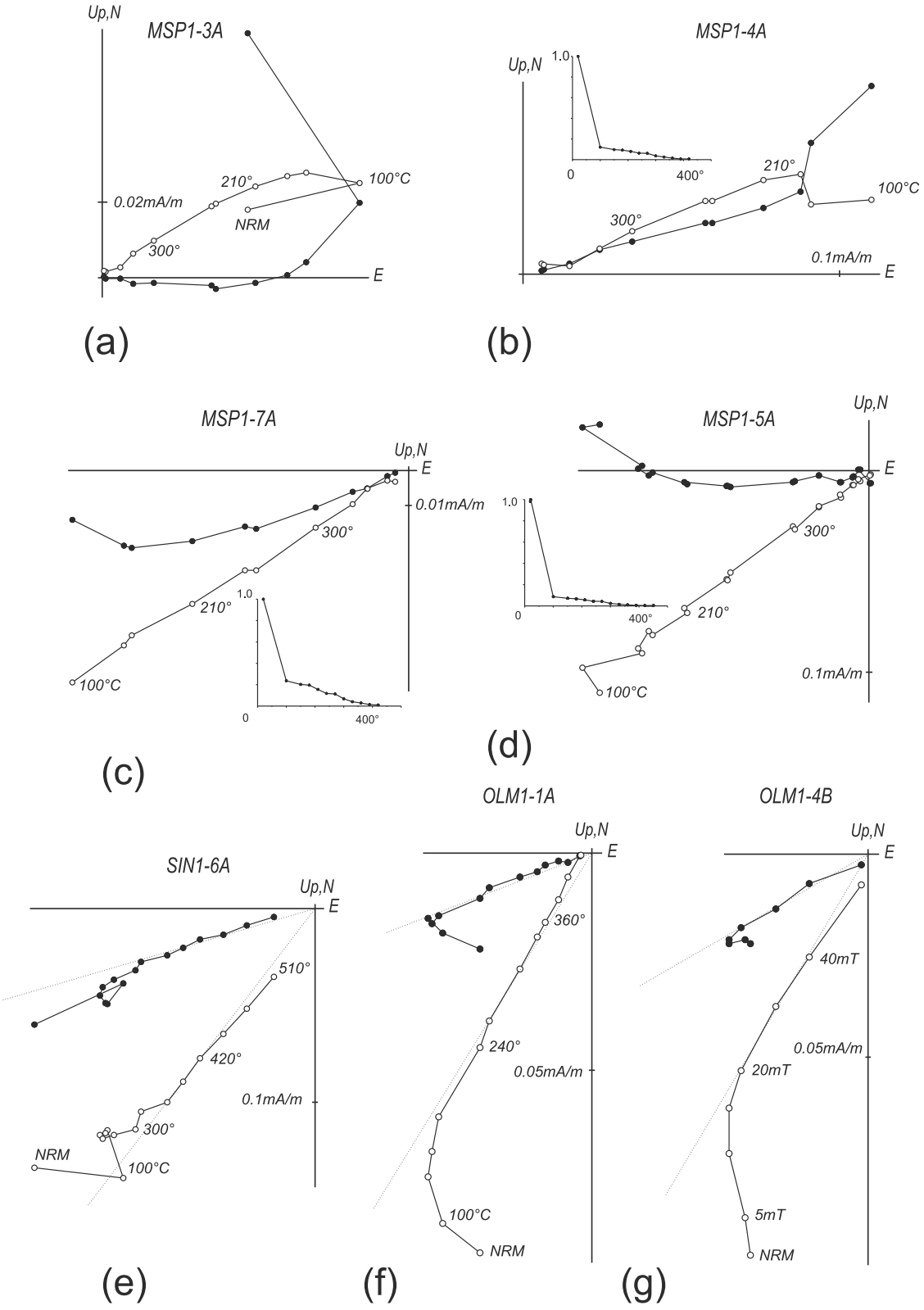

Figure 5. Results of (a–f) thermal and (g) alternating field demagnetization experiments plotted as orthogonal vector diagrams [*Zijderveld*, 1967] in stratigraphic coordinates using the paleomagnetic software of *Wack* [2010]. Solid and open dots represent vector endpoints projected onto the horizontal and vertical planes, respectively. In Figures 5b–5d, for clarity, high natural remanent magnetization values due to strong viscous components are not plotted.

Table 2. Paleomagnetic Directions From Jurassic Sediments of the Nurra Region[a]

				In Situ				Bedding Corrected			
Site	Age	N	P	D (deg)	I (deg)	k	α_{95} (deg)	D (deg)	I (deg)	k	α_{95} (deg)
OLM	L	5/9	N	286.6	50.9	169.7	5.9	243.4	58.3	196.7	5.9
CAS[b]	M	1/7	N	7.2	60.1			18.1	29.7		
CAM	M	2/6	M	280.3	39.4	658.6	9.7	259.9	57.6	658.5	9.7
CAM[b]	M	2/6	N	334.4	38.1			351.8	56.6		
CCU1[b]	E	3/6	N	347.0	51.8	19.7	47.7	9.9	62.8	19.7	47.7
CCU2[b]	M	3/5	N	15.0	62.5	1513.1	17.1	328.9	76.3	1507.7	17.1
CCU3	M	1/7	N	261.2	55.3			245.5	63.0		
CCU4	M	2/3	N	258.6	16.5			247.9	24.3		
GRI	M	5/10	N	288.4	50.2	263.5	4.7	278.0	25.3	263.5	4.7

[a]Site, sampling sites; E, Early; M, Middle; L, Late Jurassic; N, number of samples used for calculating site mean directions/number of measured samples; P, magnetic polarity (N, normal; M, mixed); D, declination; I, inclination; k, Fisher precision parameter [*Fisher*, 1953]; α_{95}, Fisher circle of 95% confidence in geographic (in situ) and bedding-corrected (TC) coordinates.
[b]Well defined paleomagnetic directions with values in geographic coordinates close to the present-day field direction.

HT component directions (maximum angular deviation values between 1.6° and 4.4° based on at least 8 demagnetization steps) that yield positive reversal and fold tests (Figure 6 and Table 4). The tilt-corrected site mean characteristic HT component direction is $D = 257.8°$ and $I = 25.6°$ ($\alpha_{95} = 10.2°$; $k = 30.5$; $N = 8$ samples, Tables 1 and 4).

4.3. Data Summary

[23] Except for two sites of Early Jurassic age, all other sites of Middle and Late Jurassic age from the four investigated regions yield reliable HTC directions (Table 5 and Figure 7). When grouped according to age, the total of 25 Middle Jurassic site mean directions from the four investigated regions show an increase of the Fisher precision parameter k from 10 to 14 after 100% tilt correction, and the reversal test after tilt correction is positive (classified as C according to the criteria of *McFadden and McElhinny* [1990]). The resulting Middle Jurassic overall mean direction is $D = 269.7°$, $I = 45.0°$, $k = 14.0$, $\alpha_{95} = 8.0°$, $n = 25$ sites.

[24] Similarly, the total of 10 Late Jurassic site mean directions from the four investigated regions show an increase of the Fisher precision parameter k from 25.3 to 45.3 after 100% tilt correction, and a positive reversal test (classified as C according to the criteria of *McFadden and McElhinny* [1990]). The resulting Late Jurassic overall

Table 3. Paleomagnetic Directions From Jurassic Sediments From the Gulf of Orosei[a]

				In Situ				Bedding Corrected			
Site	Age	N	P	D (deg)	I (deg)	k	α_{95} (deg)	D (deg)	I (deg)	k	α_{95} (deg)
OLI1	M	2/5	N	267.7	11.2	16.5	14.1	279.2	34.9	16.5	14.1
OLI2[b]	M	3/6	M	111.1	−16.6	12.6	12.7	124.7	−26.7	12.6	12.7
OLI3	M	4/8	N	277.4	37.2	13.9	19.3	279.0	52.1	13.9	19.3
ULA1[c]	M	3/8	M	249.2	40.5	22.0	16.6	249.2	40.5	22.0	16.6
ULA2	M	6/7	M	93.2	−46.0	140.4	5.8	94.6	−49.8	140.4	5.8
URZ	L	3/6	N	279.6	30.1	5.6	42.8	278.0	39.9	22.0	27.0
RIF[c]	L	7/7	M	259.3	47.3	9.4	16.0	276.2	51.8	9.4	16.0
CAL	L	5/6	M	287.5	14.9	20.8	14.9	285.7	46.8	20.8	14.9
BAU1[d]	M	4/7	N	352.9	56.7	34.5	15.9	351.9	46.5	35.0	15.8
BAU2	M	5/8	N	280.4	46.7	11.7	24.0	294.3	59.8	11.8	11.8
BUE1[d]	M	6/9	N	332.7	31.0	45.0	10.3	319.7	−10.6	37.6	11.3
BUE2	M	7/23	M	113.0	−24.2	40.1	14.8	113.1	−20.1	40.1	14.8
BUE2[d]	M	13/23	N	352.2	52.2	18.3	10.1	48.8	50.3	17.1	10.5
OHE[d]	M	3/5	N	331.5	55.6	46.6	18.3	9.1	61.1	46.6	18.3
GOR1	L	3/5	N	215.7	57.4	21.4	27.3	268.8	38.2	21.8	21.8
GOR2	L	1/3	N	259.0	32.4			277.7	56.5		
GOR2[d]	L	2/3	N	4.8	57.7	589.5	10.3	23.1	32.9	589.5	10.3
TIS1	L	2/4	N	292.7	19.9	59.0	33.1	302.3	43.8	59.0	20.0
TIS2	L	7/8	N	271.2	32.8	50.1	8.6	282.1	55.3	65.8	7.5
TIS3	L	5/8	N	268.7	20.4	77.9	8.7	268.0	51.4	77.9	8.7
SIN	L	5/7	N	269.6	45.4	55.7	10.3	262.4	55.9	49.6	11.0
LUL	M	2/6	N	270.4	12.9	1061.8	171.9	265.4	31.5		
LUL[d]	M	2/6	N	339.7	44.1	24.2	53.2	1.2	58.5	24.2	53.2

[a]Site, sampling sites; M, Middle; L, Late Jurassic; N, number of samples used for calculating site mean directions/number of measured samples; P, magnetic polarity (N, normal; M, mixed); D, declination in degrees; titI, inclination in degrees; k, Fisher precision parameter [*Fisher*, 1953]; α_{95}, Fisher circle of 95% confidence in geographic in situ and bedding-corrected coordinates.
[b]Biased direction of Jurassic mean (this study) with component of present-day field direction of the study area.
[c]Paleomagnetic mean direction calculated by combining linear trajectories of demagnetization paths with remagnetization circles, using the technique of *McFadden and McElhinny* [1988].
[d]Well defined paleomagnetic directions with values in geographic coordinates in vicinity to the present-day field, supposing an overprint of the magnetic signal.

Table 4. Paleomagnetic Directions From Jurassic Sediments of Barbagia-Sarcidano and Sulcis Regions[a]

				In Situ				Bedding Corrected			
Site	Age	*N*	P	*D* (deg)	*I* (deg)	*k*	α_{95} (deg)	*D* (deg)	*I* (deg)	*k*	α_{95} (deg)
Barbagia and Sarcidano Regions											
BSM[b]	M	5/20	M	44.0	−20.0	88.6	8.2	41.0	−22.2	88.6	8.2
CAN1[b]	M	3/6	N	314.1	46.0	1127.5	19.8	314.1	46.0	1127.5	19.8
CAN2[c]	M	5/7	M	293.5	44.4	12.6	23.0	278.3	38.4	12.6	23.0
CAN3[c]	M	4/6	R	78.1	−41.3	26.8	11.4	73.1	−33.7	26.8	11.4
MSA1	M	10/10	M	288.2	55.6	9.7	15.7	294.1	58.9	9.7	15.7
MSA2	M	5/6	R	105.5	−54.6	29.0	14.5	94.4	−53.9	29.0	14.5
MSA3	M	6/7	R	86.6	−47.3	34.7	10.7	85.3	−44.6	34.7	10.7
PER1	M	5/10	M	81.9	−50.1	24.5	16.2	75.4	−43.5	24.5	16.2
PER2	M	11/12	M	96.5	−60.8	61.4	6.0	86.2	−47.6	61.4	6.0
VNT[c]	M	3/6	M	243.2	63.8	13.4	30.0	238.1	44.2	13.4	30.0
SUL[b]	M	6/11	M	139.7	−60.3	66.4	31.2	139.7	−60.3	66.4	31.2
SAD[c]	M	5/15	M	269.6	58.0	44.9	11.9	265.3	62.3	44.9	11.9
Sulcis Region											
MSP	M	8/9	M	93.0	65.9	7.9	21.0	257.8	25.6	30.5	10.2

[a]Site, sampling sites; M, Middle; L, Late Jurassic; *N*, number of samples used for calculating site mean directions/number of measured samples; P, magnetic polarity (N, normal; R, reversed; M, mixed); *D*, declination in degrees; *I*, inclination in degrees; *k*, Fisher precision parameter [*Fisher*, 1953]; α_{95}, Fisher circle of 95% confidence in geographic (in situ) and bedding-corrected (TC) coordinates.
[b]Biased direction of Jurassic mean (this study) with component of present-day field direction of the study area.
[c]Paleomagnetic mean direction calculated by combining linear trajectories of demagnetization paths with remagnetization circles, using the technique of *McFadden and McElhinny* [1988].

mean direction is $D = 275.5°$, $I = 50.7°$, $k = 45.3$, $\alpha_{95} = 7.2°$, $n = 10$ sites.

[25] It has to be noted, that Nurra and Sulcis Regions might contain uncertainties, originated from insufficient statistical coverage of several sites and/or areas. To improve the spatial distribution, site mean directions obtained from only one or two samples are included in the study. This might obscure a regional systematic deviation in the order of some 10°. However, excluding all site mean directions based on less than three samples would bias the overall mean directions for Middle and Late Jurassic rocks only by less than 5° (Middle: $\Delta D = 2.4°$, $\Delta I = 0.5°$, Late: $\Delta D = 4.0°$, $\Delta I = 0.4°$).

[26] The resulting Middle and Late Jurassic paleopole positions plot at Lat = 16.5°, Long = 299.1° (dp = 6.4°, dm = 10.1°) and at Lat = 23.4°, Long = 301.2° (dp = 6.5°, dm = 9.7°), respectively. These results indicate a pretilting origin of the characteristic component directions retrieved in the Jurassic carbonates and for substantial tectonic coherence of the four investigated areas with only minor amounts of

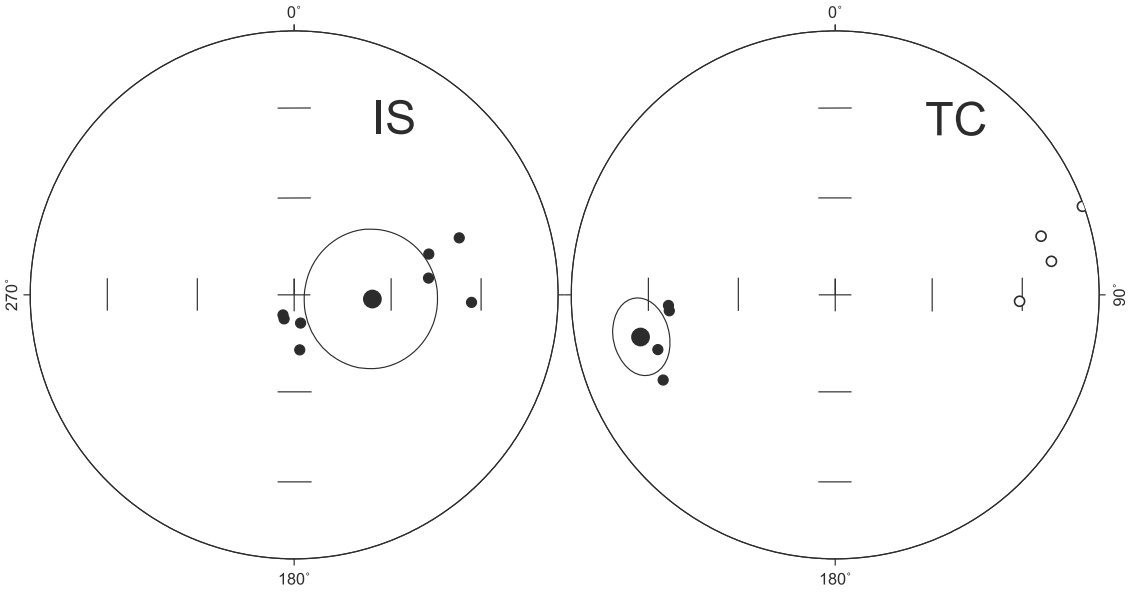

Figure 6. Stereoplots of individual sample directions of site MSP in the southwest of Sardinia in geographic in situ (IS) and stratigraphic tilt-corrected (TC) coordinates. Solid and open dots represent projection on the upper and lower hemispheres, respectively. Large black dots indicate site mean direction with 95% confidence circles (α_{95}).

Table 5. Overall Site Mean Directions[a]

Region	Jurassic Age	N	In Situ			Bedding Corrected		
			D (deg)	I (deg)	α_{95} (deg)	D (deg)	I (deg)	α_{95} (deg)
Nurra Region	Middle	4	268.7	41.2	23.7	259.4	43.4	27.7
	Late	1	286.6	50.9	5.9	243.4	58.3	5.9
Supramonte-Baronie	Middle	8	275.8	30.1	13.4	277.1	41.2	15.0
	Late	9	269.5	34.8	14.1	278.2	49.4	6.7
Barbagia-Sarcidano	Middle	12	273.2	53.5	11.6	273.2	49.7	12.3
Sulcis	Middle	1	93.0	65.9	21.0	257.8	25.6	10.2
Mean	Middle	25	273.9	46.0	9.5	269.7	45.0	8.0
	Late	10	271.9	36.6	13.0	275.5	50.7	7.2

[a]N, number of sites used for calculating overall mean directions; D, mean declination; I, mean inclination; α_{95}, Fisher circle of 95% confidence [*Fisher*, 1953] in degrees in in situ coordinates and after bedding correction.

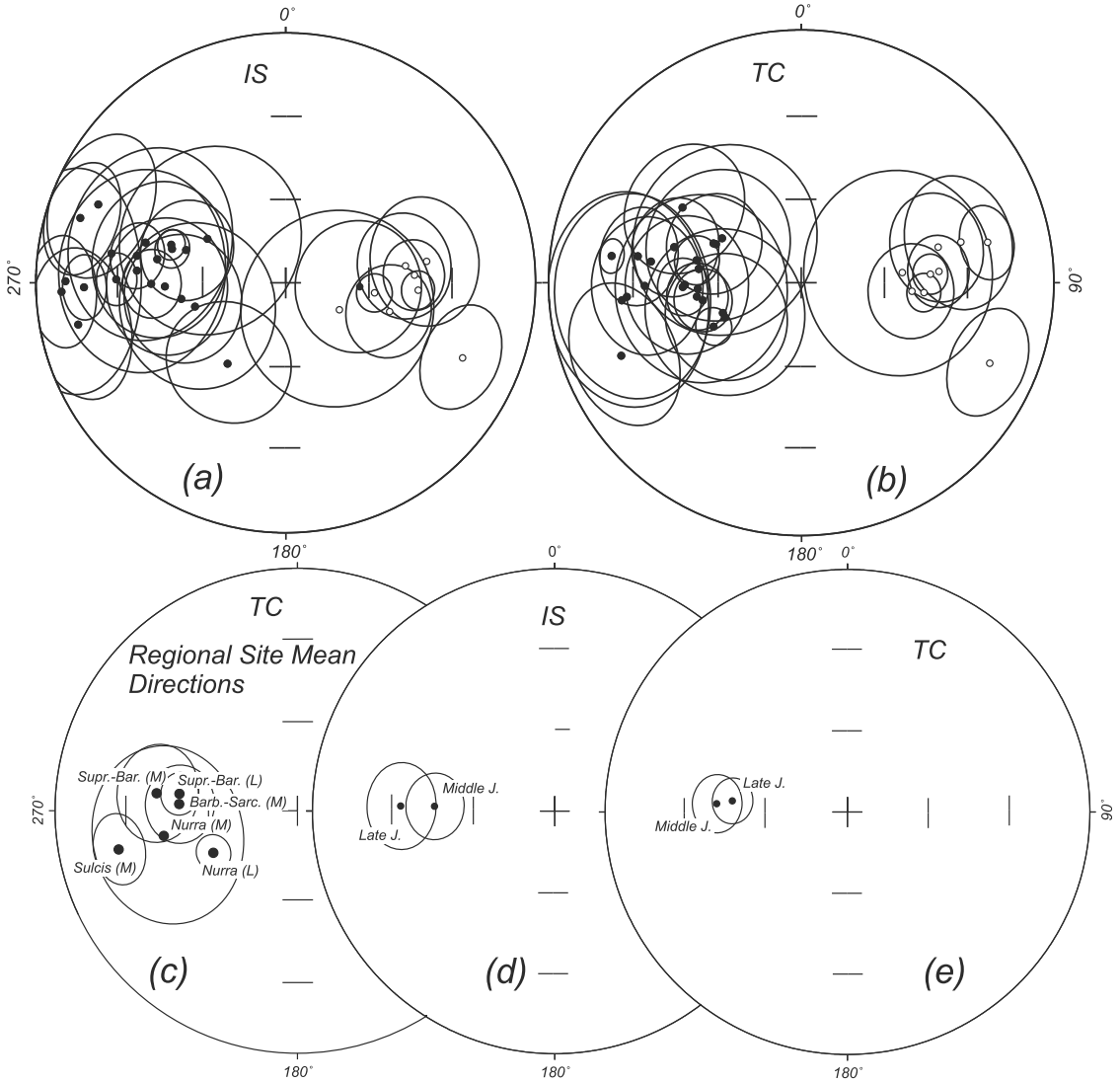

Figure 7. Stereographic projection (a, b) of all site mean directions, (c) grouped by region and age, and (d, e) according to age only. IS refers to in situ data, and TC refers to tilt-corrected data. Shown also are 95% confidence circles. Solid and open dots represent projection on the upper and lower hemispheres, respectively. Regional site mean directions are shown in Figure 7c for Supramonte-Baronie (Supr.-Bar.), Barbagia-Sarcidano (Barb.-Sarc.), and Sulcis and Nurra regions for Middle (M) and Late (L) Jurassic age.

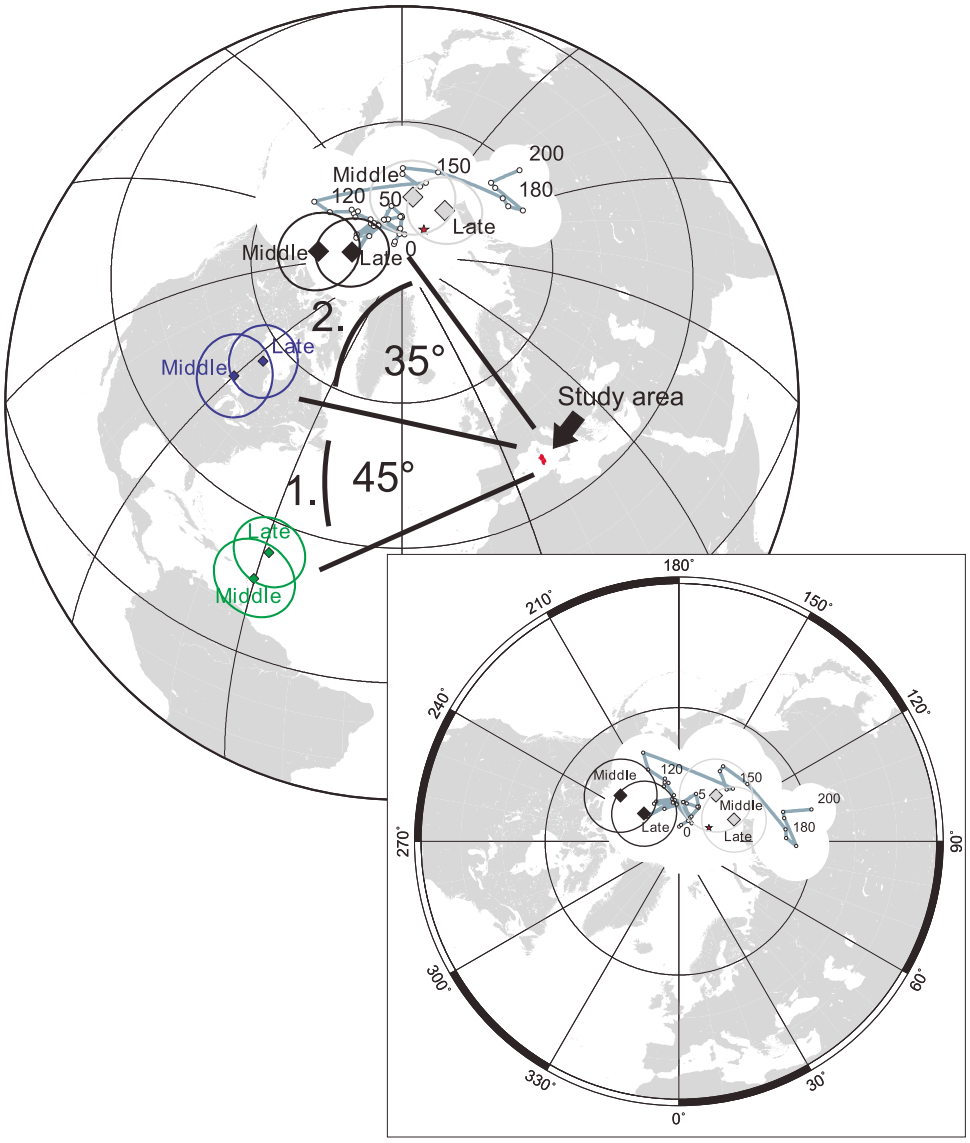

Figure 8. Paleomagnetic poles with associated α_{95} circles of confidence calculated from the overall mean Middle and Late Jurassic directions of Sardinia (green diamonds) have been rotated by closing the Liguro-Provençal Basin using rotation parameters of *Gattacceca et al.* [2007] (blue diamonds) and the Bay of Biscay using rotation parameters of *Van der Voo* [1969] (black diamonds). Gray diamonds represent poles, corrected for the opening of the Bay of Biscay with a overestimated rotation amount (60°). The apparent polar wander path of Europe with associated α_{95}s for the last 200 Myr [*Besse and Courtillot*, 2002] is indicated by open circles. The red star indicates the present-day geomagnetic north pole.

possible internal post-Jurassic rotations of ±10° (Figure 7 and Table 5).

5. Discussion and Conclusions

[27] Paleomagnetic analysis of Middle and Late Jurassic sedimentary rocks from 44 sites, sampled in four regions of Sardinia (Nurra, Baronie-Supramonte, Barbagia-Sarcidano and Sulcis) reveals the presence of reliable characteristic component directions carried essentially by magnetite. The uniform distribution of directional data from all over Sardinia and especially around the arc shaped Gulf of Orosei, yields no evidence for oroclinal bending as proposed by *Helbing et al.* [2006]. No correlation between deviation in strike and declination [*Schwartz and Van der Voo*, 1983] was identified when analyzing the directional data from Baronie and Supramonte (Figure 9).

[28] Coherent site mean directions obtained from the characteristic magnetization components allow to calculate Middle and Late Jurassic regional mean directions which are statistically indistinguishable and result in the corresponding Middle and Late Jurassic paleopoles.

[29] Middle and Late Jurassic Sardinian paleopoles were rotated into European coordinates by closing the Liguro-Provençal Basin and the Bay of Biscay using rotation parameters of *Gattacceca et al.* [2007] and *Van der Voo* [1969] assuming a two step rigid body model. In a first step a rotation was applied to close the younger Liguro-Provençal

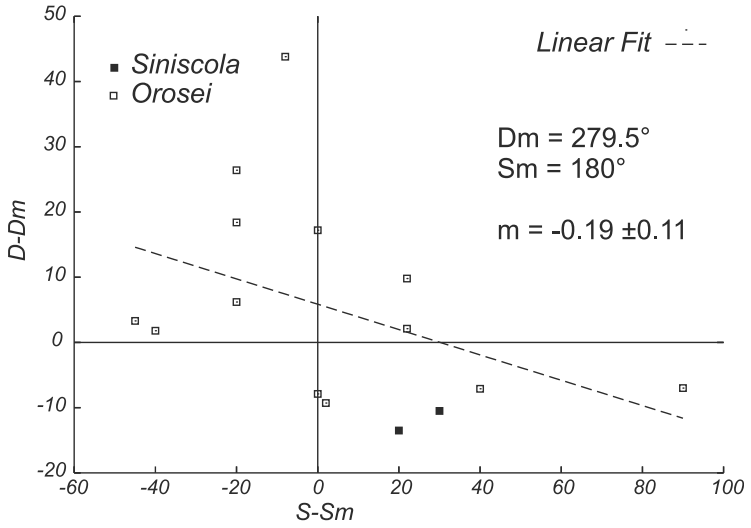

Figure 9. Deviations from mean values of declination (Dm) versus strike (Sm) for the data from the Gulf of Orosei (Supramonte). The linear fit shows no correlation between strike and declination and therefore suggests that no oroclinal bending is present in the area (method after *Schwartz and Van der Voo* [1983]).

Basin about an Euler pole located at Lat = 43.5°, Long = 9.5°, and a clockwise angle of rotation of 45° [*Gattacceca et al.*, 2007], followed by a second rotation closing the older Bay of Biscay with an Euler pole located at Lat = 43.0°, Long = −2°, and a clockwise angle of rotation of 35° [*Van der Voo*, 1969; *Gong et al.*, 2008]. The rotated paleopoles were then compared to the coeval paleopoles of the apparent polar wander (APW) path of Europe of *Besse and Courtillot* [2002]. Inspection of Figure 8 reveals that the imposed rotations bring the Sardinian paleopoles very close to the European APW path, a relatively limited statistical discrepancy seems however to persist between the rotated Sardinian paleopoles and the coeval ∼170–140 Ma poles of Europe. An explanation for this discrepancy might be an underestimation of the assumed rotation angle for the Sardinian microblock during the opening of the Bay of Biscay. Assuming a larger angle of rotation in the order of ∼60° and a similar pole of rotation would decrease the displacement of the Middle and Late Jurassic poles of Sardinia and the coeval poles of Europe (shaded poles in Figure 8). Alternatively, the Middle and Late Jurassic reference paleopoles of Europe are misplaced insofar as they are based on paleopole entries from limestones from central Europe that have an ambiguous smeared distribution with a suspicion of remagnetization, as extensively discussed by *Muttoni et al.* [2005].

[30] Acknowledging these uncertainties, the following conclusions can be drawn:

[31] 1. Only negligible amounts of differential block rotations occurred within Sardinia since the Jurassic.

[32] 2. There is no oroclinal bending in the Gulf of Orosei as proposed by *Helbing et al.* [2006].

[33] 3. Sardinia as a whole shows clear tectonic coherence with Europe during the Jurassic, and subsequently underwent a first counterclockwise rigid body rotation (juxtaposed to Iberia) during the opening of the Bay of Biscay [*Van der Voo*, 1969; *Cohen*, 1981; *Olivet*, 1996] in the Aptian [*Gong et al.*, 2008], and a subsequent counterclockwise rotation (jointly together with Corsica) during the opening of the Liguro-Provençal Basin in the Miocene [*Gattacceca et al.*, 2007].

[34] 4. As a consequence of the internal tectonic coherence of Sardinia since the Middle Jurassic, the timing of large differential rotations of up to 110° found in Permian rocks from different regions of Sardinia [*Edel et al.*, 1981; *Edel*, 2000; *Moser et al.*, 2005; *Emmer et al.*, 2005] are constrained to a generic Permian–Early Jurassic age. These large internal rotations can therefore neither be due to extensional tectonics at the European margin during the Jurassic [*Zattin et al.*, 2008], nor to Alpine tectonics that started broadly in the Late Cretaceous [*Rosenbaum et al.*, 2002], nor to subduction-related oroclinal bending in the Cenozoic [*Helbing et al.*, 2006] (Figure 9), nor to, finally, Cenozoic transcurrent tectonics [*Carmignani et al.*, 1994]. Consequently, the internal rotations observed in Permian units must have taken place in Permian-Triassic times, after the end of the Variscan orogeny and well before the Jurassic opening of the Penninic Ocean and its subsequent closure during the Alpine orogeny.

[35] The post-Variscan period was one of intense crustal reorganization in transtensional and/or transpressional tectonic regimes. During the latest Carboniferous and Early Permian, the convergence of Gondwana and Laurussia changed from oblique collision to dextral translation along continental-scale dextral shear systems linked by secondary sinistral shears that developed in Europe and North Africa between the Uralides in the east and the Appalachians in the west [*Arthaud and Matte*, 1977; *Blès et al.*, 1989; *Ziegler and Dëzes*, 2006; *McCann et al.*, 2006; *Cassinis et al.*, 2011]. This period of wrench tectonics may have culminated with the transformation of Pangea from a Pangea "B" configuration to a Pangea "A2" configuration that took place mostly during the Middle Permian [e.g., *Muttoni et al.*, 2003, 2009, and references therein]. Sardinia and Corsica, together with the Little and Great Kabylie, and the Calabria basement, were members of the same Alboran microplate [*Rosenbaum et al.*, 2002], which was attached to the French-Catalan margin prior to Alpine-Apennine deformation in the

Cenozoic [*Westphal et al.*, 1973, 1976; *Arthaud and Matte*, 1977]. They were therefore located just where most of the inferred shearing between Gondwana and Laurussia is expected to have taken place. We therefore speculate that post-Variscan intra-Pangea wrenching and shearing may have induced the large-scale rotations of fault-bounded blocks observed in Permian units of Sardinia as well as elsewhere in Europe, e.g., in the Saint-Affrique and Brive basins of the French Massif Central [*Chen et al.*, 2006], as preliminarily discussed by *Emmer et al.* [2005]. This inference, which remains at present speculative, however, will be explored in detail in a paleomagnetic work (now in progress) on Late Paleozoic–Middle Triassic rocks of Sardinia, which we consider as geological key witnesses of a major African-European contact zone.

[36] **Acknowledgments.** We thank the Editor André Revil, J.-B. Edel, A. Smirnov, and one anonymous reviewer for their very constructive comments on the manuscript. An earlier version was read by D. Bilardello and his comments lead to a significant improvement of the manuscript. Support in the field by M. Hackl is gratefully acknowledged. The study was funded by a research grant (Ba1210/8-1) to V.B. from the German Research Funding Agency (DFG).

References

Alvarez, W., S. Franks, and A. Nairn (1973), Palaeomagnetism of Plio-Pleistocene basalts from northwest Sardinia, *Nature*, *243*, 10–11.

Arthaud, F., and P. Matte (1977), Late Palaeozoic strike-slip faulting in southern Europe and northern Africa: Result of a right-lateral shear zone between the Appalachians and the Urals, *Geol. Soc. Am. Bull.*, *88*, 1305–1320.

Barca, S., and L. Costamagna (1997), Compressive "Alpine" tectonics in Western Sardinia (Italy): Geodynamic consequences, *C. R. Acad. Sci., Ser. IIa Sci. Terre Planetes*, *325*, 791–797.

Besse, J., and V. Courtillot (2002), Apparent and true polar wander and the geometry of the geomagnetic field over the last 200 Myr, *J. Geophys. Res.*, *107*(B11), 2300, doi:10.1029/2000JB000050.

Blès, J., D. Bonijoly, and C. C. Y. Gros (1989), Successive post-Variscan stress fields in the French Massif Central and its borders (Western European plate): Comparison with geodynamic data, *Tectonophysics*, *169*, 79–111.

Carmignani, L., R. Carosi, L. Disperati, A. Funedda, G. Musumeci, S. Pasci, and P. Pertusati (1992), Tertiary transpressional tectonics in NE Sardinia, Italy, in *Contributions to the Geology of Italy With Special Regard to the Paleozoic Basements*, edited by L. Carmignani and F. Sassi, pp. 45–62, Int. Geol. Correl. Prog., Paris.

Carmignani, L., S. Barca, L. Disperati, P. Fantozzi, A. Funedda, G. Oggiano, and S. Pasci (1994), Tertiary compression and extension in the Sardinian basement, *Boll. Geofis. Teor. Appl.*, *36*, 45–62.

Cassinis, G., L. Cortesogno, L. Gaggero, P. Pittau, A. Ronchi, and E. Sarria (1999), Late Palaeozoic continental basins of Sardinia, paper presented at International Field Conference on The Continental Permian of the Southern Alps and Sardinia (Italy), Regional Reports and General Correlations, Earth and Sci. Dep., Pavia Univ., Brescia, Italy.

Cassinis, G., C. Perotti, and A. Ronchi (2011), Permian continental basins in the Southern Alps (Italy) and peri-Mediterranean correlations, *Int. J. Earth Sci.*, doi:10.1007/s00531-011-0642-6, in press.

Chen, Y., B. Henry, M. Faure, J.-F. Becq-Giraudon, J.-Y. Talbot, L. Daly, and M. L. Goff (2006), New Early Permian paleomagnetic results from the Brive basin (French Massif Central) and their implications for Late Variscan tectonics, *Int. J. Earth Sci.*, *95*, 306–317.

Cherchi, A., L. Simone, R. Schroeder, G. Carannante, and A. Ibba (2010), I sistemi carbonatici giurassico-cretacei della Nurra (Sardegna settentrionale), *Geol. Field Trips*, *2*, 55–122.

Cohen, C. (1981), Plate tectonic model for the Oligo-Miocene evolution of the western Mediterranean, *Tectonophysics*, *68*, 283–311.

Cortesogno, L., G. Cassinis, G. Dallagiovanna, L. Gaggero, G. Oggiano, A. Ronchi, S. Seno, and M. Vanossi (1998), The Variscan post-collisional volcanism in Late Carboniferous-Permian sequences of Ligurian Alps, Southern Alps and Sardinia (Italy): A synthesis, *Lithos*, *45*, 305–328.

Costamagna, L. (2000), Analisi di facies della successione triassico-giurassica di Porto Pino (Sardegna sud-occidentale), *Atti Ticinesi Sci. Terra*, *41*, 65–82.

Costamagna, L., and S. Barca (2004), Stratigrafia, analisi di facies, paleogeografia ed inquadramento regionale della successione giurassica dell'area dei Tacchi (Sardegna Orientale), *Boll. Soc. Geol. Ital.*, *123*, 477–495.

Costamagna, L., S. Barca, and L. Lecca (2007), The Bajocian-Kimmeridgian Jurassic sedimentary cycle of eastern Sardinia: Stratigraphic, depositional and sequence interpretation of the new Baunei Group, *C. R. Geosci.*, *339*, 601–612, 2007.

Dieni, I., and F. Massari (1986), Mesozoic of dastern Sardinia, in *19th Micropaleontological Colloquium, Guide-Book*, edited by A. Cherchi, pp. 66–77, Soc. Paleontol. Ital., Sardinia, Italy.

Dieni, I., J. Fischer, F. Massari, M. Salard-Cheboldaeff, and C. Vozenin-Serra (1983), La succession de Genna Selole (Baunei) dans le cadre de la paléogéographie mésojurassique de la Sardaigne orientale, *Mem. Sci. Geol.*, *36*, 117–148.

Dieni, I., F. Massari, and J. Médus (2008), Age, depositional environment, and stratigraphic value of the Cuccuru 'e Flores conglomerate: Insight into the Palaeogene to Early Miocene geodynamic evolution of Sardinia, *Bull. Soc. Geol. Fr.*, *179*, 51–72, 2008.

de Jong, K., M. Manzoni, T. Stavenga, F. van Dijk, R. van der Voo, and J. Zijderveld (1973), Palaeomagnetic evidence for rotation of Sardinia during early Miocene, *Nature*, *243*, 281–283.

Edel, J.-B. (2000), Hypothèse d'une ample rotation horaire tardi-varisque du bloc Maures-Estérel-Corse-Sardaigne, *Geol. Fr.*, *1*, 3–19.

Edel, J. B., R. Montigny, and R. Thuizat (1981), Late Paleozoic rotations of Corsica and Sardinia: New evidence from paleomagnetic and K/Ar studies, *Tectonophysics*, *79*, 201–223.

Emmer, B., V. Bachtadse, G. Muttoni, A. Ronchi, and D. V. Kent (2005), Paleomagnetism of Late Paleozoic dyke swarms from Sardinia, *Eos Trans. AGU*, *86*(52), Fall Meet. Suppl., Abstract GP11A-0015.

Faccenna, C., F. Speranza, F. D'Ajello Caracciolo, M. Mattei, and G. Oggiano (2002), Extensional tectonics on Sardinia (Italy): Insights into the arc–back-arc transitional regime, *Tectonophysics*, *356*, 213–232.

Ferrandini, J., J. Gattacceca, M. Ferrandini, A. Deino, and M. Janin (2003), Chronostratigraphie et paléomagnétisme des dépôts Oglio-Miocènes de Corse: Implications géodynamiques pour l'ouverture du bassin liguro-provençal, *Bull. Soc. Geol. Fr.*, *174*, 357–371.

Fisher, R. (1953), Dispersion on a sphere, *Proc. R. Soc. London, Ser. A*, *217*, 295–305.

Gattacceca, J., A. Deino, R. Rizzo, D. Jones, B. Henry, B. Beaudoin, and F. Vadeboin (2007), Miocene rotation of Sardinia: New paleomagnetic and geochronological constraints and geodynamic implications, *Earth Planet. Sci. Lett.*, *258*, 359–377.

Gong, Z., C. Langereis, and T. Mullender (2008), The rotation of Iberia during the Aptian and the opening of the Bay of Biscay, *Earth Planet. Sci. Lett.*, *273*, 80–93.

Helbing, H., W. Frisch, P. D. Bons, and J. Kuhlemann (2006), Tension gash-like back-arc basin opening and its control on subduction rollback inferred from Tertiary faulting in Sardinia, *Tectonics*, *25*, TC4008, doi:10.1029/2005TC001904.

Horner, F., and W. Lowrie (1981), Paleomagnetic evidence from Mesozoic carbonate rocks for the rotation of Sardinia, *J. Geophys.*, *49*, 11–19.

Jadoul, F., A. Lanfranchi, C. Casellato, F. Berra, and E. Erba (2010), I sistemi carbonatici giurassici della Sardegna orientale (Golfo di Orosei), *Geol. Field Trips*, *2*, 6–54.

Kirschvink, J. (1980), The least squares lines and plane analysis of paleomagnetic data, *Geophys. J. R. Astron. Soc.*, *62*, 699–718.

Krasa, D., K. Petersen, and N. Petersen (2007), Variable field translation balance, in *Encyclopedia of Geomagnetism and Paleomagnetism*, edited by D. Gubbins and E. Herrero-Bervera, pp. 97–99, Springer, Dordrecht, Netherlands.

Manzoni, M. (1975), Paleomagnetic data from tertiary volcanics of the Campidano and associated grabens, Sardinia, *Earth Planet. Sci. Lett.*, *27*, 275–282.

McCann, T., C. Pascal, M. Timmerman, P. Krzywiec, J. López-Gómez, A. Wetzel, C. Krawczyk, H. Rieke, and J. Lamarche (2006), Post-Variscan (end carboniferous-Early Permian) basin evolution in western and central Europe, *J. Geol. Soc.*, *32*, 355–388.

McFadden, P., and M. McElhinny (1988), The combined analysis of remagnetization circles and direct observations in palaeomagnetism, *Earth Planet. Sci. Lett.*, *87*, 161–172.

McFadden, P., and M. McElhinny (1990), Classification of the reversal test in paleomagnetism, *Geophys. J. Int.*, *130*, 725–729.

Montigny, R., J. Edel, and R. Thuizat (1981), Oligo-Miocene rotation of Sardinia: K-Ar ages and paleomagnetic data of Tertiary volcanics, *Earth Planet. Sci. Lett.*, *54*, 261–271.

Moser, E., V. Bachtadse, D. Kent, G. Muttoni, and A. Ronchi (2005), Paleomagnetism of Permian sediments and volcanic rocks from Sardinia, *Eos Trans. AGU*, *86*(52), Fall Meet. Suppl., Abstract GP11A-0014.

Muttoni, G., D. V. Kent, E. Garzanti, P. Brack, N. Abrahamsen, and M. Gaetani (2003), Early Permian Pangea B to Late Permian Pangea A, *Earth Planet. Sci. Lett.*, *215*, 379–394.

Muttoni, G., E. Erba, D. Kent, and V. Bachtadse (2005), Mesozoic Alpine facies deposition as a result of past latitudinal plate motion, *Nature*, *434*, 59–63.

Muttoni, G., M. Gaetani, D. Kent, D. Sciunnach, L. Angiolini, F. Berra, E. Garzanti, M. Mattei, and A. Zanchi (2009), Opening of the Neo-Tethys Ocean and the Pangea B to Pangea A transformation during the Permian, *GeoArabia*, *14*(4), 17–48.

Oggiano, G., A. Funedda, L. Carmignani, and S. Pasci (2009), The Sardinia-Corsica microplate and its role in the Northern Apennine Geodynamics: New insights from the Tertiary intraplate strike-slip tectonics of Sardinia, *Boll. Soc. Geol. Ital.*, *128*, 527–539.

Olivet, J.-L. (1996), La cinématique de la plaque ibérique, *Bull. Cent. Rech. Explor. Prod. Elf Aquitaine*, *20*, 131–195.

Pasci, S., G. Oggiano, and A. Funedda (1998), Rapporti tra tettonica e sedimentazione lungo le fasce trascorrenti oligo-aquitaniane della Sardegna NE, *Boll. Soc. Geol. Ital.*, *117*, 443–453.

Posenato, R., L. Simone, M. Urlichs, and A. Ibba (2002), The Ladinian Muschelkalk of Punta del Lavatoio (Alghero, NW Sardinia), *Rend. Soc. Paleont. Ital.*, *1*, 283–291.

Ronchi, A., E. Sarria, and J. Broutin (2008), The"Autuniano Sardo": Basic features for a correlation through the Western Mediterranean and Paleoeurope, *Boll. Soc. Geol. Ital.*, *127*, 655–681.

Rosenbaum, G., G. Lister, and C. Duboz (2002), Relative motions of Africa Iberia, and Europe during Alpine orogeny, *Tectonophysics*, *359*, 117–129.

Rossi, P., G. Oggiano, and A. Cocherie (2009), A restored section of the "southern Variscan realm" across the Corsica-Sardinia microcontinent, *C. R. Geosci.*, *341*, 224–238.

Schwartz, S. Y., and R. Van der Voo (1983), Paleomagnetic evaluation of the orocline hypothesis in the central and southern Appalachians, *Geophys. Res. Lett.*, *10*, 505–508.

Van der Voo, R. (1969), Paleomagnetic evidence for the rotation of the Iberian peninsula, *Tectonophysics*, *7*, 5–56.

Vigliotti, L., W. Alvarez, and M. O. McWilliams (1990), No relative rotation detected between Corsica and Sardinia, *Earth Planet. Sci. Lett.*, *98*, 313–318.

Wack, M. (2010), A new software for the measurement of magnetic moments using SQUID and spinner magnetometers, *Comput. Geosci.*, *36*, 1178–1184.

Westphal, M., C. Bardon, A. Bossert, and R. Hamzeh (1973), A computer fit for Corsica and Sardinia against Southern France, *Earth Planet. Sci. Lett.*, *18*, 137–140.

Westphal, M., J. Orsini, and P. Vellutini (1976), Le microcontinent corso-sarde, sa position initiale: Donnees paléomagnétiques et raccords géologiques, *Tectonophysics*, *30*, 141–157.

Zattin, M., F. Massari, and J. Médus (2008), Thermochronological evidence for Mesozoic-Tertiary tectonic evolution in the eastern Sardinia, *Terra Nova*, *20*, 469–474, 2008.

Ziegler, P., and P. Dëzes (2006), Crustal evolution of Western and Central Europe, *Geol. Soc. Spec. Publ.*, *32*, 43–56.

Zijderveld, J. D. (1967), A. C. demagnetization of rocks: Analysis of results, in *Methods in Paleomagnetism*, edited by D. W. Collinson, K. M. Creer, and S. K. Runcorn, pp. 254–286, Elsevier, Amsterdam.

Zijderveld, J. D., K. A. De Jong, and R. Van der Voo (1970), Rotation of Sardinia: Palaeomagnetic evidence from Permian rocks, *Nature*, *226*, 993–994.

K. Aubele, V. Bachtadse, and U. Kirscher, Geophysics, Department of Earth and Environmental Sciences, Munich University, Theresienstr. 41, D-80333 Munich, Germany. (aubele@geophysik.uni-muenchen.de; valerian@lmu.de; kirscher@geophysik.uni-muenchen.de)

G. Muttoni, Department of Earth Sciences, University of Milan, via Mangiagalli 34, I-20133 Milan, Italy. (giovanni.muttoni1@unimi.it)

A. Ronchi, Department of Earth Sciences, University of Pavia, via Ferrata 1, I-27100 Pavia, Italy. (luigiausonio.ronchi@unipv.it)